

Preparation and Characterization of Supported Mixed Metal Oxides: Thermal Decomposition of Heteropoly Metal Complexes Immobilized on Silica

ROBERT K. BECKLER¹ AND MARK G. WHITE²

School of Chemical Engineering, Georgia Institute of Technology, Atlanta, Georgia 30332-0100

Received October 15, 1987; revised February 2, 1988

Supported mixed metal oxides were prepared by the temperature-programmed decomposition of a highly characterized system of silica-immobilized heteropoly complexes containing Cu(II) and M(III) ($M(\text{III}) = \text{Al, Cr, Fe}$). The investigation focused on two main aspects of the thermal degradation: a study of the decomposition path and characterization of the resultant samples. The decomposition process, monitored *in situ* by thermogravimetric analysis, infrared spectroscopy, and mass spectrometry, appeared to lead to the formation of mixed oxides with a stoichiometry of $M\text{Cu}_3\text{O}_{7.5}$. Electron microscopy showed sintering of the oxides into particles which contain Cu and M. The population of these particles increased with increasing temperature. Selective chemisorptions of NH_3 , CO, and NO indicated that temperature of decomposition affects active site densities. In particular, it was observed that conditions for the decomposition could be selected to maximize the activation of metal oxide sites by complex decomposition yet minimize the deactivation by sintering of supported oxide particles. © 1988 Academic Press, Inc.

INTRODUCTION

A number of investigators have recently focused attention on the potential of supported complexes as precursors to highly dispersed metal or metal oxide catalysts (1-5). Conventional deposition techniques, such as adsorption of metal salts or ions from solution, depend on many complicating factors, including concentration, adsorption rate, and precipitant affinity for the support (6). Chemically immobilized complexes, on the other hand, provide an even initial dispersion of precursor on the support. In these cases, by modifying both complex structure and support surface character, researchers may gain better control of particle size, structure, and dispersion following activation by thermal decomposition (1-5).

A majority of the reported studies have examined thermal decomposition of sup-

ported mononuclear complexes (1-5). Previously, we reported the characterization of a series of heteropolynuclear coordination compounds of the form $M[(\mu\text{-OH})\text{Cu}(\mu\text{-OCH}_2\text{CH}_2\text{NEt}_2)]_6^{3+}$ ($M(\text{III}) = \text{Al, Cr, Fe}$) which ion exchanged to a monolayer coverage on silica (Cab-O-Sil) (7). A fundamental investigation was developed to prepare and characterize supported mixed metal oxides formed by pyrolysis of these immobilized $M(\text{III})/\text{Cu}(\text{II})$ complexes. This article describes a series of experiments designed to study the decomposition, including influences of procedural conditions on the pathway to metal oxide formation, and characterization of the resultant samples.

EXPERIMENTAL

Preparation of supported $M[(\mu\text{-OH})\text{Cu}(\mu\text{-OCH}_2\text{CH}_2\text{NEt}_2)]_6^{3+}$. Heteropoly complexes of the form $M[(\mu\text{-OH})\text{Cu}(\mu\text{-OCH}_2\text{CH}_2\text{NEt}_2)]_6^{3+}$ ($M(\text{III}) = \text{Al, Cr, Fe}$) were ion exchanged to Grade M-5 Cab-O-Sil ($\sim 200 \text{ m}^2/\text{g}$, Cabot Corp.) by adsorption from acetonitrile as reported carrier (7). In this study, monolayer loadings of

¹ Present address: Westvaco Charleston Research, P.O. Box 5209, Charleston, SC 29406.

² To whom all correspondence should be addressed.

250 $\mu\text{mole complex/g Cab-O-Sil}$ (approx. 28 wt%) were used throughout.

Thermal decomposition. Samples of supported $M(\text{III})/\text{Cu}(\text{II})$ complex were decomposed by temperature-programmed decomposition (TPDE) (15°C/min from 150°C to final temperature, then held 30 min) in a flowing dry N_2 atmosphere. Samples decomposed to 250, 300, 350, and 450°C were prepared for investigation of temperature effects.

Gravimetric analysis of thermal decomposition. The thermal decomposition of supported complexes was studied gravimetrically using a Perkin-Elmer TGS-2 thermogravimetric analyzer (TGA) system (see (18, 19) for description of system). To observe weight loss vs temperature, fresh samples (~ 10 mg) were equilibrated for 1 h at 150°C in either dry N_2 or air flowing at 200 ml/min and then heated at a constant rate of 15°C/min to 450°C. Final weight was recorded at 150°C after the sample had been allowed to equilibrate with humidified air (to rehydrate the support). The recorded weight loss curves (150–450°C) were corrected for support dehydration assuming a constant rate of H_2O removal between 150 and 450°C.

Mass spectrometry analysis of thermal decomposition. All samples were analyzed in a VGZAB-E mass spectrometer system. The sample off-gases were ionized by electron impact at 70 eV. A sample of supported complex was prepared for TPDE in a mass spectrometer by heating under vacuum (150°C, 3 h, 10^{-6} Torr). A small sample (~ 2 mg) was introduced to the spectrometer sample chamber and equilibrated in flowing UHP He (150°C, 10 min). A programmed rate of 15°C/min was initiated, and spectra of the off-gases ($m/e = 30\text{--}150$) were recorded up to 300°C.

IR spectroscopy analysis of thermal decomposition. The decomposition of supported complexes was studied by IR spectroscopy as a function of temperature in a Perkin-Elmer 281-B IR spectrometer (see (18, 19) for details of the system). Self-sup-

porting sample wafers (20 mm in diameter, 50 mg weight) decomposed at 250, 300, 350, and 450°C (inert atmosphere) were loaded into a large-volume gas cell equipped with CaF_2 windows (25 \times 2 mm). The IR analysis was conducted at room temperature under vacuum (10^{-6} Torr). All spectra were recorded in the absorbance mode for double-beam IR path.

Surface area measurements. Surface areas for the decomposed samples were determined according to the static BET technique using N_2 (Matheson, 99.999%) physisorption at 77 K. Samples were pretreated by evacuation at 10^{-6} Torr and heating to 250°C for 1.5 h.

Electron microscopy analysis. SEM analysis was performed using a Cambridge Stereoscan 150 microscope equipped with a LaB_6 electron source (212 kV) and a Tracor X-ray detector for energetic dispersive analysis of X-rays (EDAX). TEM analysis was conducted with a Philips transmission electron microscope (20-kV W source).

Samples of supported complex (decomposed at 300, 350, and 450°C) were prepared for scanning electron microscope (SEM) according to the following procedure. Sample (~ 10 mg) was suspended in distilled H_2O (10 ml) and dispersed ultrasonically. A drop of this suspension was applied to a thin polyethylene film and allowed to air dry. The film was then coated by a carbon overlayer (vacuum deposition, 2×10^{-5} Torr) to prevent charge buildup on the specimen in the beam. For transmission electron microscopy, samples (~ 10 mg) were hypersonically dispersed in distilled H_2O (10 ml). Albumin-coated copper grids were dipped in the suspension and allowed to air dry.

Selective chemisorption of NH_3 , CO, and NO—gravimetric analysis. Surface characterization by selective chemisorption of NH_3 , CO, and NO was studied gravimetrically using the TGA system described earlier. Typical procedure involved drying the sample in a dry stream of N_2 (400 ml/min) at

mild temperatures for 1 h (125°C for NH₃, 80°C for CO and NO), exposure to adsorbate in N₂ at the drying temperature (1 h, 30 Torr NH₃, 15 Torr CO, 5 Torr NO), and then N₂ purge (1 h). Residual adsorbate in the presence of the inert purge at the drying temperature was defined as chemisorbed species. Gases, including N₂ (HoloX), NH₃ (99.99%, Matheson), CO (99.99%, Matheson), and NO (5.04%, bal. N₂, Matheson), were dried on delivery to the TGA sample chamber by passage across beds of activated sieves.

Selective chemisorption of NH₃, CO, and NO—Infrared spectroscopy. Sorptions of NH₃, CO, and NO were studied by IR spectroscopy using the same CaF₂ window, double-beam sample cell and IR spectrometer as described earlier. The samples were treated with the gases before the spectra were recorded at room temperature under vacuum (10⁻⁶ Torr). Typical procedure for chemisorption on wafers of decomposed sample required equilibration with adsorbate (1 h, 125°C, and 30 Torr for NH₃, 80°C and 15 Torr for CO, 80°C and 5 Torr for NO), followed by evacuation (10⁻⁶ Torr) at the same temperature (30 min). Residual adsorbate in the vacuum was defined as the chemisorbed phase. Gases (same as in gravimetric study) were dried over activated sieves.

RESULTS

Gravimetric Analysis of Thermal Decomposition

Decomposition of the supported complexes was studied gravimetrically in both N₂ and air to investigate the effects of temperature and gas exposure on weight loss. Reported in Fig. 1A is a plot of sample weight (W) vs temperature (T) in an N₂ atmosphere for $M(\text{III}) = \text{Fe}$. A plot of dW/dT vs T (Fig. 1B) revealed three minima at 225, 250, and 310°C. When heated to 450°C, the sample achieved a final weight loss of 12.4% (corrected for support dehydration). A similar study conducted in air yielded the

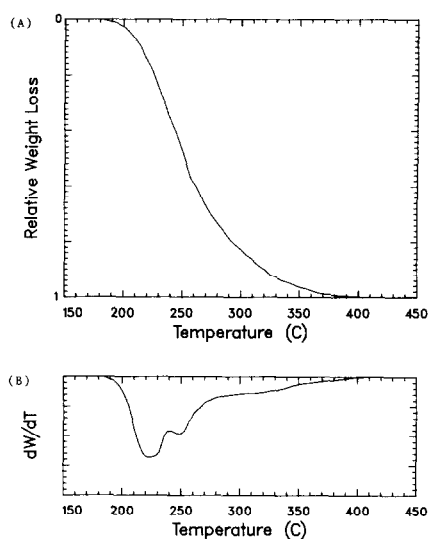


FIG. 1. Temperature-programmed decomposition of supported $M(\text{III}) = \text{Fe}$ complex in a N₂ atmosphere. (A) W vs T . Weight loss (W) is expressed on a relative basis such that the percentage of ultimate weight loss may be read as a function of T . Weight loss due to support dehydration was corrected as described under Experimental. (B) dW/dT vs T . This first derivative plot reveals three minima at 225, 250, and 310°C. The plot is portrayed only qualitatively to illustrate subtle transition regions.

same final weight loss. Throughout the remainder of this study, all thermal decompositions were conducted either in an inert atmosphere or under vacuum.

Mass Spectrometry Analysis of Thermal Decomposition

Conditions of the TGA decomposition ($M(\text{III}) = \text{Fe}$) in an inert atmosphere (15°C/min) were duplicated in a mass spectrometer sample chamber for analysis of the volatilized components as a function of temperature. Portrayed in Fig. 2 are instantaneous scans ($m/e = 30\text{--}120$) for volatiles from a sample heated to 200 and 256°C. In the two spectra, base peaks of 86 and 44 were obtained, respectively, with other primary peaks positioned at increments of 14 relative to the base peaks. In all scans, no significant peaks were obtained above an m/e of 120.

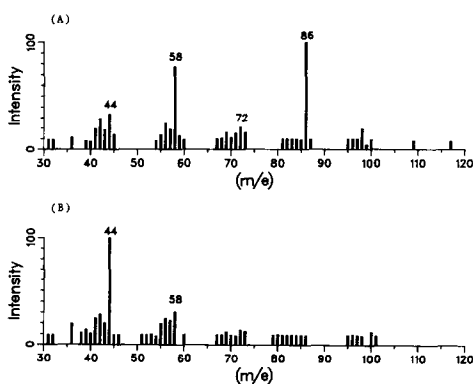


FIG. 2. Mass spectra of species volatilized by decomposition as a function of temperature ($M(\text{III}) = \text{Fe}$). (A) 200°C. From Fig. 1A, it is estimated that 4% of total weight loss has occurred at this temperature. (B) 256°C. Sixty-three percent of total weight loss realized.

Infrared Spectroscopy Analysis of Thermal Decomposition

IR spectra of fresh, supported $M(\text{III}) = \text{Fe}$ complex and samples heated to temperatures of 250, 300, 350, and 450°C are reported in Fig. 3. With heating to 250°C, the CH stretching vibrations (2970–2860 cm^{-1}) and HCH deformations (1450 and 1380

cm^{-1}) associated with the *N,N*-diethylaminoethoxy ligands decreased significantly, and by 300°C disappeared entirely. A sharp peak at 3740 cm^{-1} formed with sample degradation (isolated hydroxyl OH stretch) and grew in intensity to 450°C, while the broad OH stretch at 3700–3200 cm^{-1} (hydrogen-bonded OH and complex bridging hydroxide) diminished with increased heat treatment.

Surface Area Measurements

Surface areas of fresh, supported $M(\text{III})$ complex samples decomposed at 250, 300, 350, and 450°C were determined according to the BET isotherm technique. These values are listed in Table 1. While apparent surface area (m^2/g total weight) increased with the progression of decomposition temperatures, specific surface area relative to the support (m^2/g Cab-O-Sil) remained essentially constant.

Electron Microscopy Analysis

Samples decomposed at 300, 350, and 450°C were examined by scanning and transmission electron microscopies to investigate differences in physical features

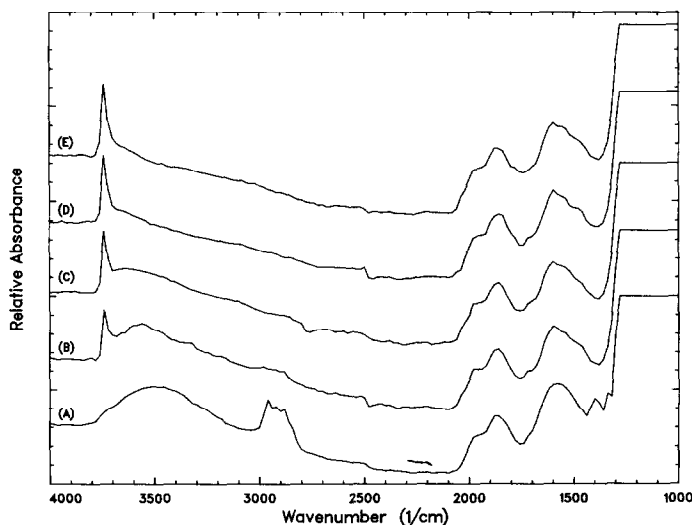


FIG. 3. IR spectra of supported $M(\text{III}) = \text{Fe}$ complex as a function of decomposition temperature. (A) No decomposition. (B) 250°C. (C) 300°C. (D) 350°C. (E) 450°C.

with varying decomposition temperature. For each sample, several parts of the surface were surveyed before a representative photograph was recorded. Of the two techniques, TEM micrographs provided the best resolution (Fig. 4). Electron transmission is least intense through the most dense regions (dark spots). Under the conditions of the microscope, features larger than 5 nm can be resolved. Numerous particles forming these darker images were noted for the samples decomposed at 350 and 450°C (Figs. 4B and 4C), while very few dark spots were observed for the 300°C sample (Fig. 4A). No clear distinction could be made between the relative particle sizes of the samples heated to 350 and 450°C.

While the resolution inherent to the SEM technique did not permit estimation of particle sizes, images could be subjected to energetic dispersive analysis of X-rays to identify compositions of the contrasting regions (Fig. 5). For the depicted $M(\text{III}) = \text{Al}$ sample, images producing the most intense backscatter yielded significant X-ray emissions characteristic of Cu (0.93, 8.05, 8.90 keV) and Si (1.84 keV), along with a weak peak attributed to Al (1.56 keV). As the beam was shifted to a less intense region, the Al peak disappeared, the Cu emissions diminished, and the Si peak intensified

TABLE 1

BET Surface Areas for Decomposed Supported $M(\text{III}) = \text{Fe}$ Complex as a Function of Temperature

Sample decomposition temperature (°C)	Apparent surface area ^a (m ² /g)	Specific surface area ^b (m ² /g Cab-O-Sil)
Not decomposed	139	194
250	157	190
300	161	188
350	170	195
450	171	195

^a Surface area expressed per total sample weight.

^b Surface area expressed per weight of Cab-O-Sil support only. The fraction of sample containing Cab-O-Sil was predicted from the gravimetric study of decomposition of a 250 $\mu\text{mole/g}$ Cab-O-Sil sample of $M(\text{III}) = \text{Fe}$ complex (Fig. 1A). Pure Cab-O-Sil gave a BET surface area of 201 m²/g.

TABLE 2

Gravimetric Analysis of NH_3 , CO, and NO Chemisorption on Supported $M(\text{III}) = \text{Fe}$ Complex as a Function of Decomposition Temperature

Sample decomposition temperature (°C)	Chemisorption ^{a,b} (mg/g Cab-O-Sil)		
	NH_3	CO	NO
Not decomposed	3.2	0	22.5
250	8.1	2.8	16.2
300	8.0	3.4	15.5
350	8.2	3.3	16.8
450	6.8	1.0	12.1

^a Chemisorption is defined as adsorbate remaining bound on the sample in the presence of a flowing N_2 purge.

^b NH_3 measurement at 125°C; CO and NO at 80°C.

markedly. Oxygen X-ray emissions could not be detected with this instrumentation.

Selective Chemisorption of NH_3 , CO, and NO—Gravimetric Analysis

Selective chemisorption of the molecules NH_3 , CO, and NO was used to probe the surface properties of the decomposed $M(\text{III}) = \text{Fe}$ samples (250, 300, 350, and 450°C). Table 2 summarizes the gravimetric chemisorption results for the decomposed samples, reported as milligrams of adsorbate per gram of Cab-O-Sil. As a basis of comparison, sorption levels are included for the fresh, supported $M(\text{III}) = \text{Fe}$ complex under similar conditions of exposure.

For NH_3 chemisorption at 125°C, the decomposed samples demonstrated an increased capacity for ammonia retention relative to the starting material. Carbon monoxide, which did not chemisorb on the intact supported complexes, adsorbed for all four decomposed samples at 80°C. Nitric oxide, however, showed a reduced affinity for the decomposed material. As indicated in Table 2, the chemisorption levels for each gas were approximately constant with temperature of decomposition, except for the 450°C sample, which revealed a clear decrease in sorption capacity.

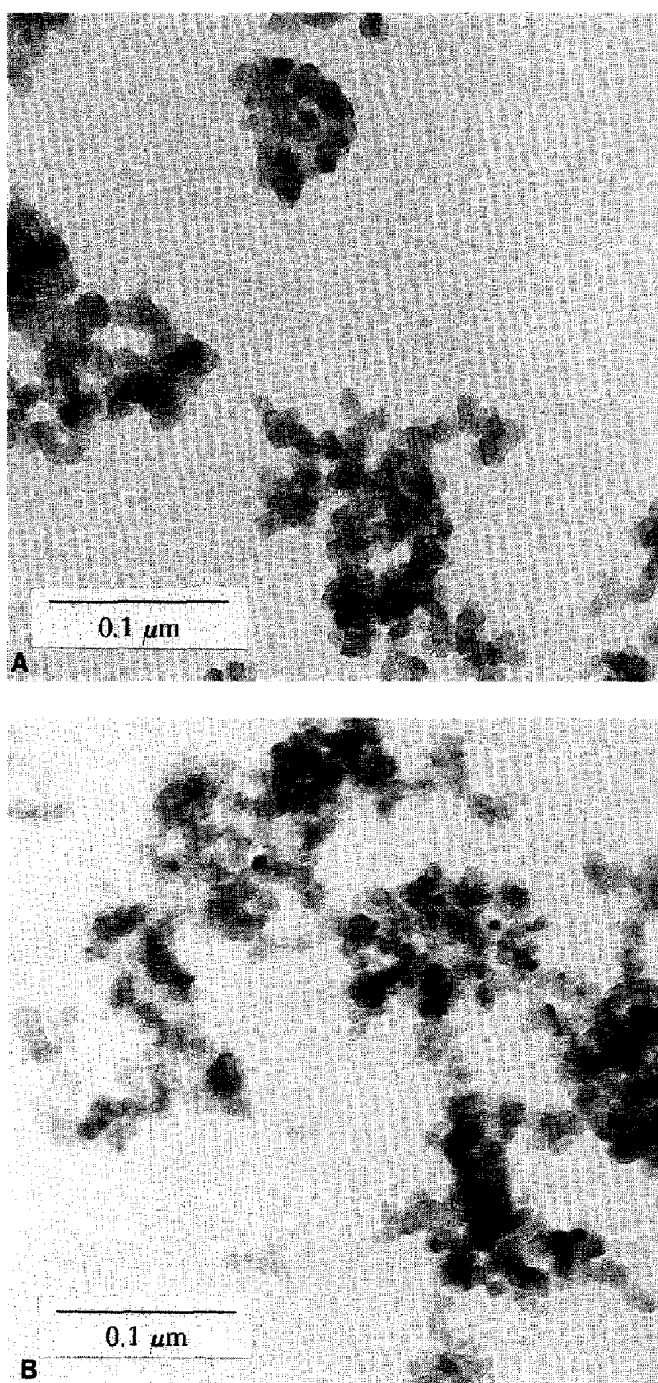


FIG. 4. TEM micrographs of thermally decomposed samples of supported $M(\text{III}) = \text{Fe}$ complex. (A) 300°C decomposition. (B) 350°C decomposition. (C) 450°C decomposition.

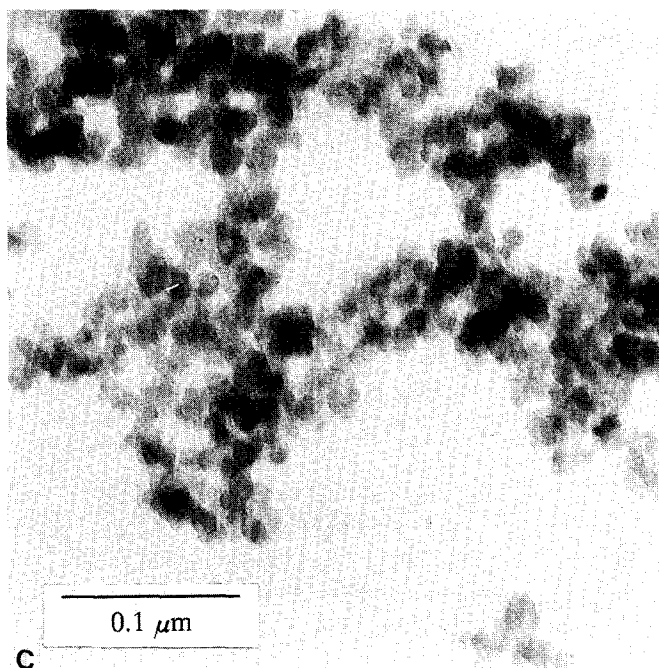


FIG. 4—Continued.

Selective Chemisorption of NH_3 , CO , and NO —Infrared Spectroscopy

The chemisorptions of NH_3 , CO , and NO were investigated by infrared spectroscopy, with adsorption conditions matching those described in the gravimetric analysis. IR spectra of NH_3 chemisorption at 125°C on samples of supported $M(\text{III}) = \text{Fe}$ complex decomposed at 250, 300, 350, and 450°C are presented in Fig. 6. Ammonia dosage produced NH stretching vibrations at 3345 and 3270 cm^{-1} and a HNH bending vibration at 1600 cm^{-1} . The intensities of these peaks were similar for the 250, 300, and 350°C samples and lower for the 450°C case. CO chemisorption at 80°C produced a single, weak vibration at 2140 cm^{-1} associated with the adsorbate carbon–oxygen stretch (Fig. 7). As a function of sample decomposition temperature, the intensity of the CO peak increased proceeding from 250 to 300°C, and then decreased with the series 300 to 350 to 450°C. Finally, the spectra for NO chemisorption at 80°C are pro-

vided in Fig. 8. With NO exposure to the decomposed samples, a number of weak vibrations were observed: 1900, 1810, 1710, and 1610 cm^{-1} . While the low intensity of

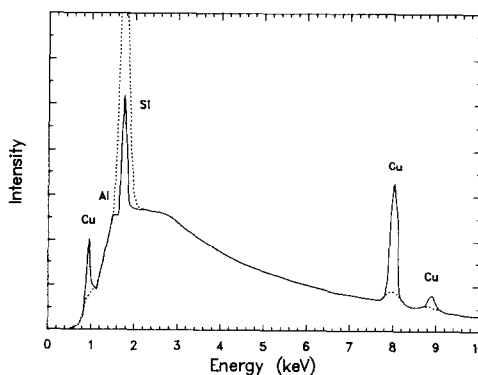


FIG. 5. Energetic dispersive analysis of X-ray emissions for decomposed $M(\text{III}) = \text{Al}$ sample (350°C). The solid curve denotes the EDAX scan of a single intense spot image (SEM mode), while the dotted curve approximates the effect of shifting the electron beam from the more intense image to a less intense region. Atomic assignments are based on the characteristic energies of X-ray emissions.

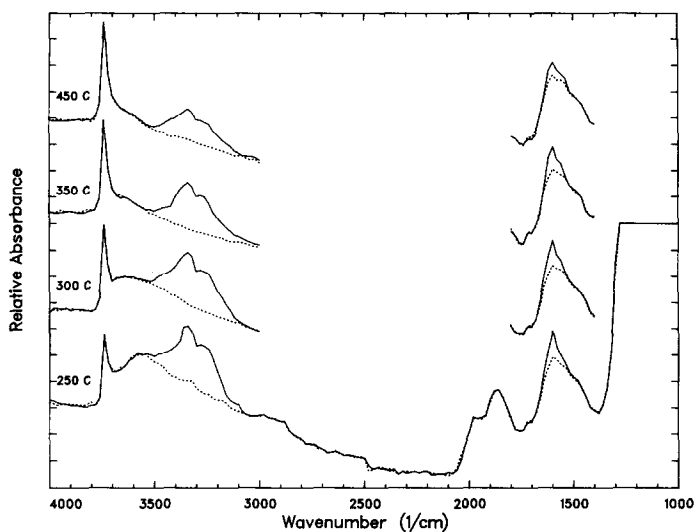


FIG. 6. IR spectra of NH_3 chemisorption on supported $M(\text{III}) = \text{Fe}$ complex as a function of decomposition temperature. Chemisorption of NH_3 , measured at 125°C , was defined as residual NH_3 remaining on the sample in a vacuum.

these peaks made it difficult to discern any trends associated with temperature of decomposition, it appeared that the NO vibrations diminished slightly over the 450°C sample.

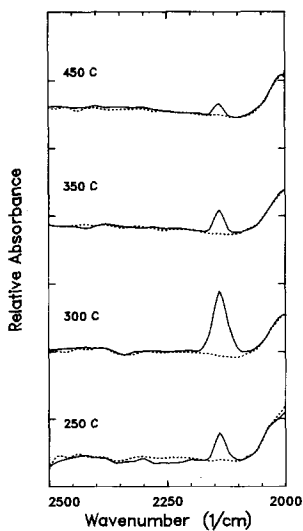


FIG. 7. IR spectra of CO chemisorption on supported $M(\text{III}) = \text{Fe}$ complex as a function of decomposition temperature. Chemisorption of CO , measured at 80°C , was defined as the residual CO remaining in the sample in a vacuum.

DISCUSSION

Gravimetric Analysis of Thermal Decomposition

The measured value of weight loss with decomposition may provide an indication of the ultimate composition remaining after

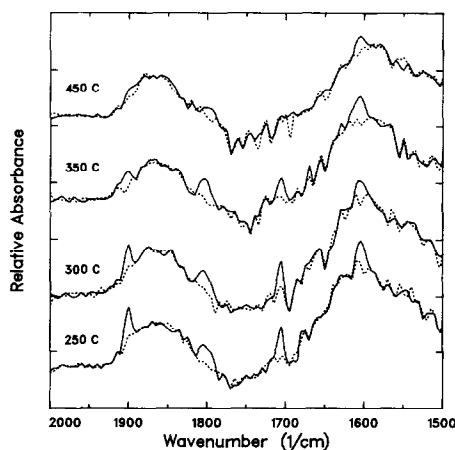


FIG. 8. IR spectra of NO chemisorption on supported $M(\text{III}) = \text{Fe}$ complex as a function of decomposition temperature. Chemisorption of NO , measured at 80°C , was defined as the residual NO remaining on the sample in a vacuum.

heat treatment to 450°C. Assuming that the complex $M[(\mu\text{-OH})\text{Cu}(\overline{\mu\text{OCH}_2\text{CH}_2\text{NEt}_2})]_6^{3+}$ degrades to the oxides of $M(\text{III})$ and $\text{Cu}(\text{II})$, the residual product would have a composition of $\text{MCu}_6\text{O}_{7.5}$. (It should be noted that the complex contains excess O atoms compared to this final oxide composition.) For $M(\text{III}) = \text{Fe}$, decomposition of a 250 $\mu\text{mole/g}$ Cab-O-Sil sample of supported complex to the product $\text{FeCu}_6\text{O}_{7.5}$ would result in a 12.9% loss in weight. This theoretical value compares with the measured 12.4% from decomposition in both air and N_2 . The presence of transitions in weight loss vs T suggested the stepwise breakdown of complex ligands as a function of temperature.

Mass Spectrometry Analysis of Thermal Decomposition

Tracing the thermal decomposition of supported $M(\text{III}) = \text{Fe}$ complex by mass spectrometry provided a means of identifying the volatiles with rising temperature. The first mass spectrum in Fig. 2 (200°C scan) resembles the fragmentation pattern of the tertiary amine: triethylamine (8). This pattern may result from degradation of the bridging N,N -diethylaminoethoxy ligands ($\mu\text{-OCH}_2\text{CH}_2\text{NEt}_2$) of the supported $M[(\mu\text{-OH})\text{Cu}(\overline{\mu\text{OCH}_2\text{CH}_2\text{NEt}_2})]_6^{3+}$ complex. Fragmentations at the alkyl groups would generate the species 14 units apart by loss of CH_2 groups. As the temperature of decomposition is increased, it is likely that some oxygen-containing fragments contribute to the spectra as well. In addition, the 256°C spectrum shows $m/e = 44$ as the base peak. While certain nitrogen- or oxygen-containing fragments may add to this peak, some carbon formation is expected with the thermal decomposition, which might combine with excess oxygen from the complex to form CO_2 . Although not reflected in the spectra of Fig. 2, H_2O is most likely evolved as well (from support dehydration).

Mass spectral interpretations of the volatilized components are more meaningful

when considered with the gravimetric temperature-dependent study of weight loss. From the plot of weight loss vs T (Fig. 1A, N_2 atmosphere), it is estimated that 4% of the total weight loss had occurred at 200°C and 63% at 256°C. From the 200°C scan, it appears that the N,N -diethylaminoethoxy ligand is first to degrade. Furthermore, the IR spectrum of the 250°C sample (Fig. 3) indicated extremely weak CH stretching vibrations, suggesting that relatively little of the N,N -diethylaminoethoxy ligand remained to contribute to the mass spectrum of 256°C.

Infrared Spectroscopy Analysis of Thermal Decomposition

IR spectroscopy not only documented the destruction of the organic portion of the supported complex with heating, but also pointed to the breakdown of the bridging hydroxide structure linking $\text{Cu}(\text{II})$ ions to the central metal ion $M(\text{III})$. The bridging OH stretch of pure $M[(\mu\text{-OH})\text{Cu}(\overline{\mu\text{OCH}_2\text{CH}_2\text{NEt}_2})]_6^{3+}$ has been observed at $\sim 3550\text{--}3500\text{ cm}^{-1}$ (9). Although obscured by the broad Cab-O-Sil OH vibration at $3700\text{--}3200\text{ cm}^{-1}$, heating to 350°C greatly decreased all vibrations in this range. Our earlier work (7) showed that the complex attached to the Cab-O-Sil by an ion-exchange mechanism between complex hydroxides and surface silanols. The disappearance of the complex OH stretch confirms not only the degradation of the precursor structure but also the destruction of the ion-exchanging link with the Cab-O-Sil surface silanols.

Electron Microscopy Analysis

Micrographs of TEM studies (Fig. 4) suggested that temperature of decomposition alters both particle size and dispersion. The few samples we photographed did not allow for a statistical analysis of the particle sizes; however, the micrographs did show qualitative changes with increasing temperature. The differences were more distinct between the cases of 300 and 350/450°C,

which revealed the appearance of larger particles as well as an increase in the concentration of visible particle formation on the support. It was difficult to ascribe significance to further changes in particle size between samples heated from 350 to 450°C.

The EDAX study of the most intense electron backscattering region (in the SEM investigation of decomposed $M(\text{III}) = \text{Al}$ complex on SiO_2) confirmed that these particles contain the greatest concentration of Cu and Al relative to the less intense gray images, which showed the highest concentration of Si. These results, combined with the gravimetric and mass spectral analyses of decomposition, suggest that the species remaining on the support surface are primarily metal oxide in composition (with a Cu to M ratio of 6:1, given the precursor complex composition).

Selective Chemisorption of NH_3 , CO , and NO

Decomposing the supported $M(\text{III}) = \text{Fe}$ complexes increased the capacity to chemisorb both ammonia and carbon monoxide. Since NH_3 is a nonselective adsorbate for Brønsted and Lewis acid sites, this result suggests that the net population of acid sites increased. The IR spectra of NH_3 sorption (Fig. 6) further revealed that if any Brønsted sites are interacting with NH_3 , the acidity is insufficient to produce NH_4^+ (evidenced by no vibration at 1450 cm^{-1} for the HNH bend of NH_4^+ (10)). In the intact complex, vacant Cu(II) sites did not chemisorb CO while the coordinatively saturated $M(\text{III})$ ion was not accessible for interaction; with decomposition, however, sites for strong CO interaction were created (Fig. 7). The CO IR stretching frequency observed at 2140 cm^{-1} compares with reported vibrations of 2140 cm^{-1} on CuO/SiO_2 (11), 2130 cm^{-1} on Cu_2O (12), 2120 cm^{-1} on Cu/SiO_2 (13), and 2172 cm^{-1} on $\text{Fe}(\text{II})/\text{SiO}_2$ (14). (Harrison and White (15) observed that surface oxygen and hydroxyls on $\text{Fe}(\text{III})/\text{SiO}_2$ tend to react with sorbed CO to form carbonate and bicarbonate with bands

of 1590 , 1305 , and 1030 cm^{-1} ; these vibrations were not observed in this study.)

Although capacity for NH_3 and CO increased by decomposing the supported $M(\text{III}) = \text{Fe}$ complexes, NO chemisorption decreased. The intact complexes have shown a high affinity for NO at the vacant Cu(II) ions as reported in Ref. (9). Thus, the degradation appears to immediately decrease the number of strong sites for NO sorption. In the IR spectra for NO exposure, bands were observed at 1900 , 1810 , 1710 , and 1610 cm^{-1} , while a single NO stretching frequency of 1890 cm^{-1} was recorded over the intact supported complex. Other studies of NO adsorption have reported the following: 1890 cm^{-1} on CuO/SiO_2 ($\text{Cu}^{2+}-\text{NO}^+$) (11); 1910 , 1810 cm^{-1} ($\text{ON}-\text{Fe}^{2+}-\text{NO}$) and 1830 , 1750 cm^{-1} ($\text{Fe}^{2+}-\text{NO}$) on reduced $\text{Fe}_2\text{O}_3/\text{SiO}_2$ (16); 1750 , 1700 cm^{-1} ($\text{ON}-\text{Fe}^{3+}-\text{NO}$) and 1820 cm^{-1} ($\text{Fe}^{3+}-\text{NO}$) on oxidized $\text{Fe}_2\text{O}_3/\text{SiO}_2$ (16); and 1590 cm^{-1} on Fe_2O_3 ($\text{Fe}^{3+}-\text{NO}^-$) (17).

The gravimetric and IR spectroscopic studies of selective chemisorption pointed to two important aspects of the decomposition investigation. First, the degradation immediately changes the chemistry of the system by destroying the bridging OH groups which saturated the $M(\text{III})$ ion, and the bridging alkoxide groups ($\mu\text{-OCH}_2\text{CH}_2\text{NEt}_2$) which linked the six Cu(II) ions. The chemisorption properties of the generated metal oxides were clearly different from those observed over the intact precursor complexes—enhanced NH_3 and CO sorptions and diminished NO pickup. Second, the ultimate number of available sites depended on the final temperature of decomposition. Evidenced in all three chemisorption studies, the quantity of active sorption sites decreased by heating from 350 to 450°C.

CONCLUSIONS

A number of experiments have been described to explore the thermal decom-

position of supported polynuclear $M(\text{III})/\text{Cu}(\text{II})$ complexes as a preparative technique for highly dispersed mixed metals or metal oxides. Gravimetric and IR spectroscopy studies of the decomposition as a function of temperature focused on the conditions necessary to achieve complete degradation. Selective chemisorptions of NH_3 , CO , and NO suggested that the residual species were primarily metal oxide in character. Electron microscopy investigations, along with gravimetric analyses of the chemisorptions, depicted the formation of larger particles of active component with rising decomposition temperature, likely decreasing the number of exposed sites for adsorption (as observed for the 450°C specimen). Collectively, the data suggest a trade-off in the progress of decomposition: conditions must be selected to achieve maximum uniform decomposition with minimal particle sintering.

As a final consideration, we place this work in a perspective relative to our previous studies of the precursor system. We have reported a series of investigations regarding the acid and catalytic behavior of the intact complexes as models of more complicated mixed oxide acids (such as silica-alumina) (9, 18–21). A high level of characterization was achieved with many of the same techniques described in this article, primarily as a result of an a priori understanding of complex structure, active site orientation, and the complex-support binding interaction. With thermal degradation of this system, however, this understanding was forfeited and the level of characterization reduced to the case of a more complicated heterogeneous system. While this comparison points to stark differences in the degree of catalyst characterization, it yet appears that highly defined immobilized complex systems may offer the most promise for gaining greater control in the development of supported mixed metals or metal oxides.

ACKNOWLEDGMENT

We gratefully acknowledge Professor J. Aaron Bertrand (School of Chemistry, Georgia Institute of Technology, Atlanta, GA 30332) for his comments and criticisms.

REFERENCES

1. Watters, K. L., Howe, R. F., Chojnacki, T. P., Fu, C. M., Schneider, R. L., and Wong, N. B., *J. Catal.* **66**, 424 (1980).
2. Bailey, D. C., and Langer, S. H., *Chem. Rev.* **81**, 109 (1981).
3. Yermakov, Yu. I., Kuznetsov, B. N., and Zakharov, V. A., "Catalysis by Supported Complexes." Elsevier, Amsterdam, 1981.
4. Lisitsyn, A. S., Golovin, A. V., Kuznetsov, V. L., and Yermakov, Yu. I., *J. Catal.* **95**, 527 (1985).
5. Iwasawa, Y., Chiba, T., and Ito, N., *J. Catal.* **99**, 95 (1986).
6. Lee, S.-Y., and Aris, R., *Catal. Rev. Sci. Eng.* **27**(2), 207 (1985).
7. Beckler, R. K., and White, M. G., *J. Catal.* **102**, 252 (1986).
8. "Eight Peak Index of Mass Spectra," 3rd ed., Vol. 1, Part 1. Royal Society of Chemistry, Nottingham, 1983.
9. Beckler, R. K., and White, M. G., *Langmuir* **3**, 1074 (1987).
10. Nakamoto, K., "Infrared and Raman Spectra of Inorganic and Coordination Complexes," 4th ed. Wiley, New York, 1986.
11. London, J. W., and Bell, A. T., *J. Catal.* **31**, 32 (1973).
12. Lokhov, Yu. A., and Davydov, A. A., *Kinet. Katal.* **20**, 1498 (1979).
13. Eischens, R. P., Pliskin, W. A., and Francis, S. A., *J. Chem. Phys.* **22**, 1786 (1954).
14. Rebenstorf, B., and Larsson, R., *Z. Anorg. Allg. Chem.* **453**, 127 (1979).
15. Harrison, P. G., and White, E. G., *J. Chem. Soc. Faraday Trans. 1* **74**, 2703 (1978).
16. Yuen, S., Chen, Y., Kubsh, J. E., Dumesic, J. A., Topsøe, N., and Topsøe, H., *J. Phys. Chem.* **86**(15), 3022 (1982).
17. Davidson, E. R., *J. Chem. Phys.* **46**, 3320 (1967).
18. Babb, K. H., and White, M. G., *J. Catal.* **98**, 343 (1986).
19. Beckler, R. K., and White, M. G., *J. Catal.* **109**, 25 (1988).
20. Beckler, R. K., and White, M. G., *J. Catal.*, in press.
21. Beckler, R. K., Ph.D. thesis, Georgia Institute of Technology, Atlanta, GA, 1987.